ISSN 0031-918X, Physics of Metals and Metallography, 2020, Vol. 121, No. 1, pp. 65–71. © Pleiades Publishing, Ltd., 2020.
Russian Text © The Author(s), 2020, published in Fizika Metallov i Metallovedenie, 2020, Vol. 121, No. 1, pp. 72–78.

STRUCTURE, PHASE TRANSFORMATIONS, AND DIFFUSION

Structure and Surface Properties of Metastable Austenitic Steel Subjected to Liquid Carburizing at a Reduced Temperature

R. A. Savrai[a, *], P. A. Skorynina[a], A. V. Makarov[a, b, c], and A. L. Osintseva[a]

[a] *Institute of Engineering Science, Ural Branch, Russian Academy of Sciences, Ekaterinburg, 620049 Russia*
[b] *Mikheev Institute of Metal Physics, Ural Branch, Russian Academy of Sciences, Ekaterinburg, 620108 Russia*
[c] *Ural Federal University Named after the First President of Russia B.N. Yeltsin, Ekaterinburg, 620002 Russia*
**e-mail: ras@imach.uran.ru*

Received July 12, 2019; revised July 23, 2019; accepted August 19, 2019

Abstract—This work investigates the effect of liquid carburizing at 780°C on the structure, chemical and phase composition, microhardness, and surface roughness of corrosion-resistant austenitic chromium-nickel steel. The depth of the carburized layer has been determined to be about 2 mm. The steel structure at a distance of 0.15 mm from the surface consists of carbon-saturated austenite γ_C, α' martensite, and fine $Cr_{23}C_6$ chromium carbides located along austenitic grain boundaries. No carbides are observed in the grain body. There are austenite γ_C and chromium $Cr_{23}C_6$ carbides in the structure at a depth from 0.15 to 2 mm. The number and the size of carbides decrease with distance from the steel surface. Carburizing increased the microhardness of the steel surface by a factor of four (from 200 to 800 HV0.025) and the roughness parameter *Ra* to 1.35 μm.

Keywords: corrosion-resistant austenitic steel, liquid carburizing, structure, phase composition, microhardness, surface roughness

DOI: 10.1134/S0031918X20010135

INTRODUCTION

Service properties of mechanical engineering products determine the state of their surface layer to a great extent, because it is the surface that is subjected to corrosive media and wearing and contact loads. The surface must therefore have a whole complex of properties, which is determined by the working conditions of the product, to ensure the necessary performance. 18Cr–10Ni austenitic stainless steels, which have become popular in manufacturing industry, have a high corrosion resistance, but low strength [1] and tribological properties [2], as well as insufficient contact endurance under cyclic impact loading [3]. An enhanced strength and wear resistance of austenitic stainless steels can be achieved by both deformation [4–8] and surface enrichment with interstitial atoms: carbon (carburizing) and nitrogen (nitriding) [9–12], or the combination of these methods (combined treatment) [13]. Carburizing in the case of austenitic chromium–nickel steels is the most preferable chemical-thermal treatment, because it allows one to form thick hardened layers, which, unlike nitrided layers, are still low-magnetic [14].

As a rule, carburizing is performed in solid, liquid, and gas carburizers at temperatures from 850°C and higher. This treatment provides a high-depth hardened layer (1 mm and more) and can be effectively implemented under modern manufacturing conditions. However, standard carburizing is typically characterized by a large amount of carbide precipitates, which deteriorates the corrosive properties of austenitic stainless steel. Low-temperature carburizing (below 500°C), which retains the corrosion properties of steel due to reduced carbide formation in the surface layer, has been actively studied in recent years [15–17]. However, a significant disadvantage of this type of carburization is the small (about 0.1 mm) depth of the hardened layer. The possible achievement of a greater hardened layer depth at a reduced carburizing temperature of 700–800°C to retain the corrosion resistance of austenitic chromium–nickel steel is therefore of great interest. Since carburizing is a diffusion process, a decrease in its temperature can significantly slow down the carbon saturation of the surface. In this case, carburizing should be carried out in a liquid carburizer, where the carbon saturation rate and the surface treatment uniformity are higher than those achieved by using other carburizers.

The work was aimed at studying the structure, chemical and phase composition, microhardness and surface roughness of austenitic steel AISI 321 subjected to liquid carburizing at a temperature of 780°C.

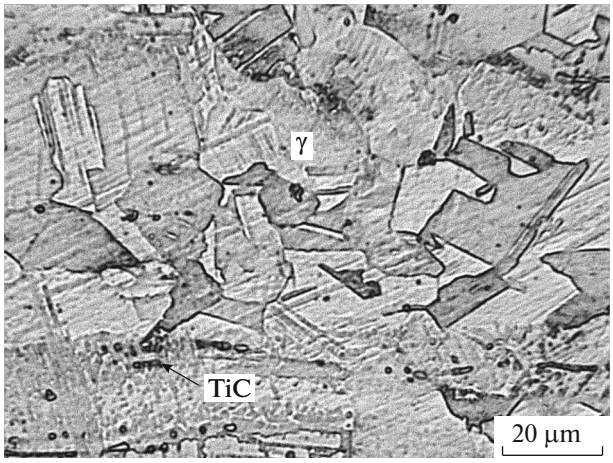

Fig. 1. Microstructure of the quenched AIS I321 steel (optical microscopy).

EXPERIMENTAL

The object under study was commercial corrosion-resistant austenite steel AISI 321 with the following chemical composition (wt %): 0.05 C, 16.80 Cr, 8.44 Ni, 0.33 Ti, 1.15 Mn, 0.67 Si, 0.26 Mo, 0.13 Co, 0.03 Nb, 0.31 Cu, 0.036 P, 0.005 S, and Fe for balance. The steel in an as-delivered state was a rolled sheet 10 mm thick. The samples prepared for carburizing were plates 52 × 40 mm in size. Heat treatment (quenching) of AISI 321 steel samples was carried under the following conditions: heating to a temperature of 1100°C, holding at this temperature for 40 minutes, and water cooling. The surface of the samples was mechanically and electrolytically polished. AISI 321 hardened steel samples were liquid carburized in a 100-mm diameter and 300-mm high crucible in a salt melt with silicon carbide (in wt %): 80% Na_2CO_3 + 10% NaCl + 10% SiC at 780°C for 15 h. After carburizing, the samples were cooled in water.

The steel microstructure after quenching was examined using a Neophot-21 optical microscope. The structure and phase composition of the steel, as well as the surface of the samples after carburizing, were investigated using a Tescan VEGA II XMU scanning electron microscope equipped with an INCA ENERGY 450 energy dispersive X-ray spectrometer. X-ray diffraction (XRD) analysis was performed on a Shimadzu XRD-7000 X-ray diffractometer in Cr $K\alpha$ radiation. The phase composition, integral width B of austenite lines $(111)_\gamma$ and $(200)_\gamma$, and dislocation density ρ were determined. The amount of α phase was calculated by formula $V_\alpha = 100/\{1 + 1.45 \times (I_{(111)\gamma}/I_{(110)\alpha})\}$, where V_α was the volume fraction of α phase (vol %) and $I_{(111)\gamma}$ and $I_{(110)\alpha}$ were the integral intensities of the γ and α phases [18]. Dislocation number density ρ was calculated using the following equation: $\rho = kB^2$, where B was the integral width of the (111)γ line (rad) and k was the constant coefficient $k = 2 \times 10^{16}$ cm^{-2} [19].

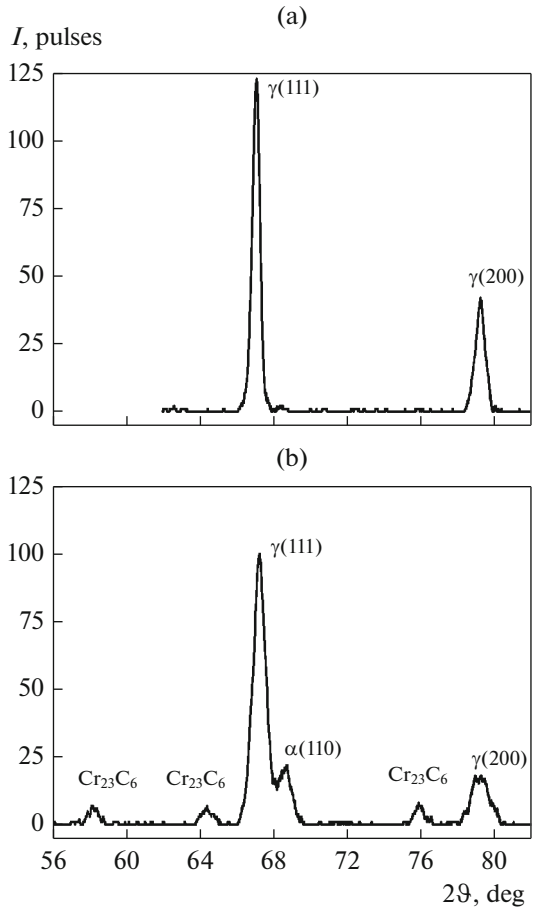

Fig. 2. X-ray diffraction patterns of the AISI 321 steel surface after (a) quenching and (b) carburizing.

Microhardness was measured by the recovered indentation method using a Shimadzu HMV-G21DT hardness tester at a load of 0.245 N for 15 s and at a loading rate of 40 μm/s. The change in the microhardness over the depth of a carburized layer was investigated on a cross section. Surface roughness parameters were determined using a Wyko NT-1100 optical profilometer.

RESULTS AND DISCUSSION

Figure 1 shows the microstructure of the AIS I321 steel after heat treatment. It consists of austenitic grains (γ phase) and some titanium carbide inclusions TiC. XRD analysis suggests that there is no α phase in the quenched steel (Fig. 2a). The microhardness of the quenched AISI 321 steel is 200 $HV_{0.025}$.

The steel structure at a distance to 0.15 mm from the surface after liquid carburizing at 780°C consists of carbon-saturated austenite γ_C, martensite, and $Cr_{23}C_6$ chromium carbides (Fig. 3), which is supported by XRD data (Fig. 2b). The amount of the α phase is 14 vol % (Table 1). There is no α phase at a distance above 0.15 mm from the surface and the structure consists of the γ_C phase and $Cr_{23}C_6$ carbides (Fig. 3a).

Carbide particles are small enough (the majority of them are smaller than 1 μm). They are concentrated along the boundaries of austenitic grains and do not exist inside the grains (see Fig. 3b). This is caused by the high atomic diffusion mobility at grain boundaries and indicates that the atomic diffusion mobility in the grain body is no longer sufficient for the carbide phase to precipitate at 780°C. Carburizing also increases the X-ray line width B of austenite $(111)_\gamma$ from 30.0 (in quenched state) to 48.4 min and $(200)_\gamma$, from 33.0 to 40.2 min (see Table 1). This is caused by crystal lattice microdistortions, which can be caused by the increased carbon content in the lattice and the growth of the number density of crystal structure defects. In particular, dislocation density ρ in the surface layer increases from 1.93×10^{12} to 3.97×10^{12} cm^{-2} as a result of carburizing (see Table 1).

The electron microprobe analysis indicates that the amount of carbon and other alloying elements in needle-shaped crystals (Fig. 4a) and outside of them (Fig. 4b) is the same in the grain body at a depth of 0.15 mm. This confirms the metallographic analysis results, which state that there is no carbide phase in the grain body, and, therefore, the observed crystals are martensite crystals. The chemical analysis of the particles located along grain boundaries (see Fig. 3b) indicates increased carbon and chromium contents (Fig. 4c), which, taking into account the X-ray analysis (see Fig. 2b), allows one to identify these particles as chromium carbides $Cr_{23}C_6$.

Martensite formation in the carburized AISI 321 steel may be due to several factors. The α-martensite formation in carburized stainless steels, such as Kh18N9T, is possible due to the precipitation of a carbide phase together with the chromium depletion of the surrounding austenitic matrix and an increase in the temperature M_s of martensitic transformation start [20]. However, Fig. 3 shows no chromium carbides in the grain body. Therefore, deformation of the austenitic matrix is the most likely reason for martensite formation. Significant thermal stresses, relaxation of which in austenitic steels can be achieved by deformation upon cooling after carburizing, are known to occur during carburizing. For example, slip bands and deformation martensite were observed in the surface layer of the AISI 304L steel after low-temperature carburizing [21]. According to some estimates, the stress level in the surface layer of the carburized steel can reach 2000 MPa [22]. The increased dislocation density in the surface layer of the AISI 321 steel, which after carburizing increases twice as much as the dislocation density in the quenched state, also indicates the previous deformation (see Table 1). Consequently, martensite formed in AISI 321 steel after carburizing

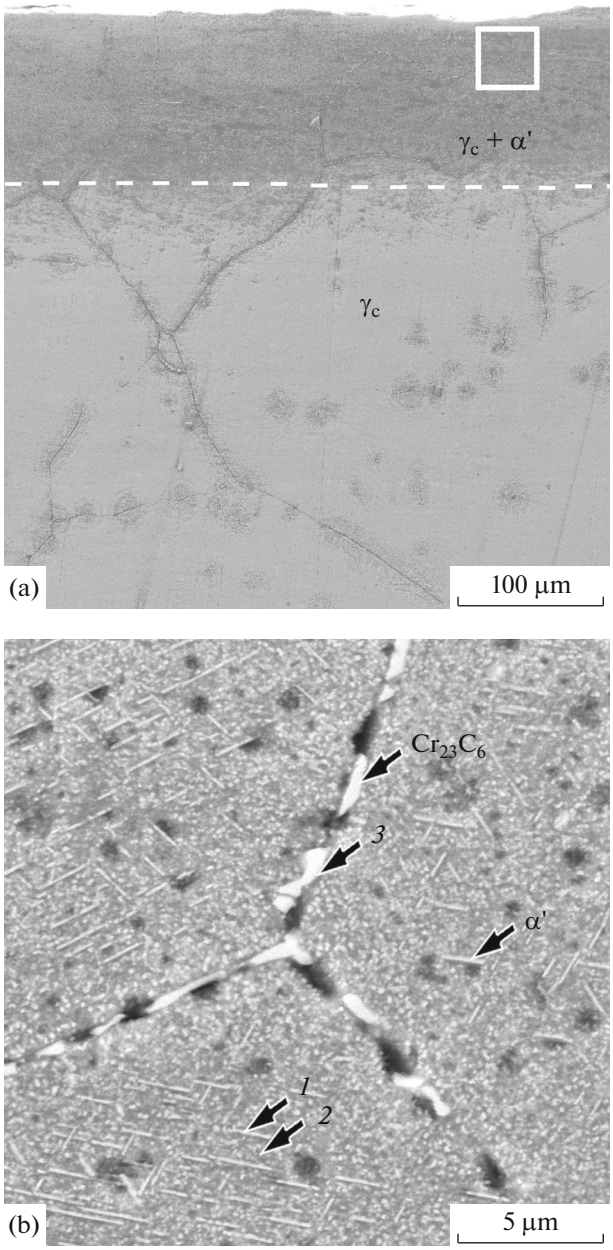

Fig. 3. Surface structure of the steel AISI 321 layer (electron scanning microscopy) after carburizing: (a) general view and (b) area indicated by the frame in Fig. 3a. Numbers *1*, *2*, and *3* indicate the areas where energy dispersive microanalysis was performed.

Table 1. Volume fraction V_α of α phase, integral width B of XRD lines (111)γ and (200)γ, and dislocation density ρ in the surface layer of the AISI 321 steel

Treatment conditions	V_α, vol %	$B_{(111)\gamma}$, min	$B_{(200)\gamma}$, min	ρ, $10^{12} \times$ cm^{-2}
Quenching	0	30.0	33.0	1.93
Carburizing	14	48.4	40.2	3.97

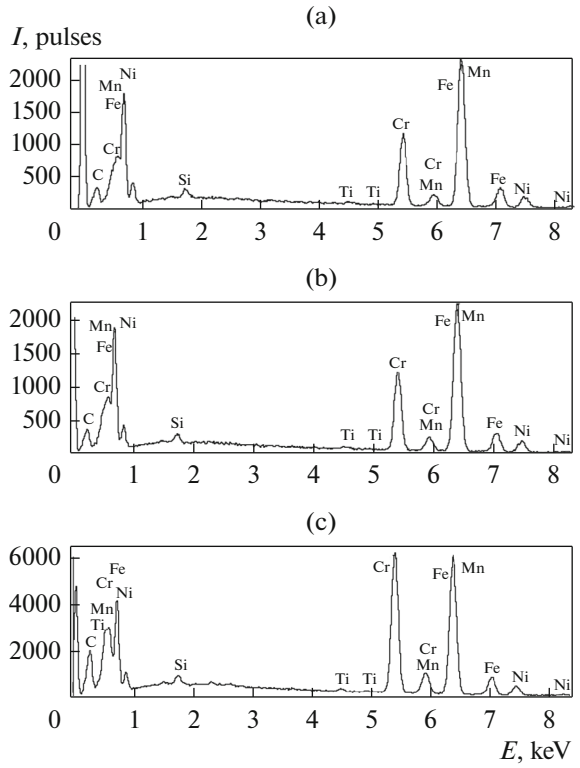

Fig. 4. Spectra of AISI 321 steel elements (energy dispersion microanalysis) after carburizing: (a) section 1, (b) section 2, and (c) section 3 in Fig. 3b.

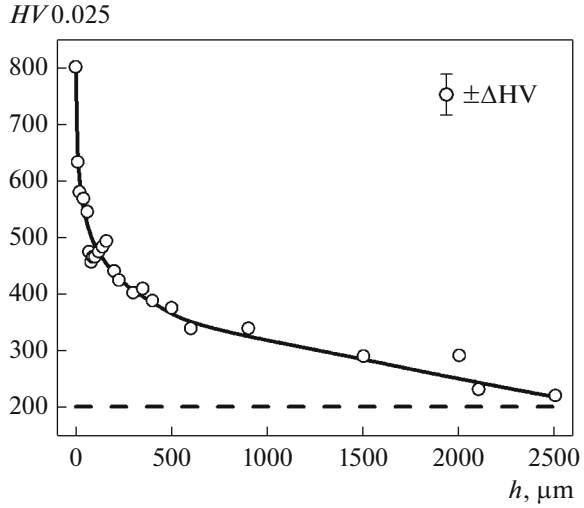

Fig. 5. Microhardness $HV_{0.025}$ of the AISI 321 steel surface layer after carburizing at depth h from the surface. The dashed line indicates the microhardness of the quenched steel.

can be considered to be of deformation origin. In addition, an austenite saturated with nitrogen or carbon (expanded austenite) is characterized by a shift of the austenite $(111)_\gamma$ and $(200)_\gamma$ lines towards smaller angles [23, 24] as compared to the position of X-ray lines in the quenched steel. Figure 2 shows no similar shift of

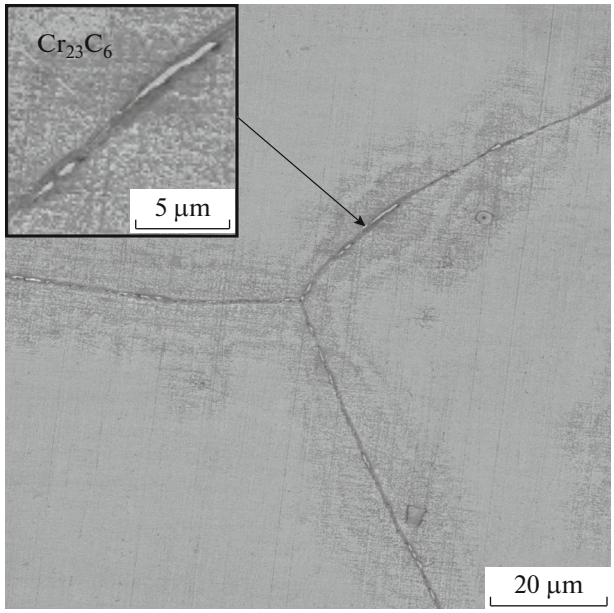

Fig. 6. Structure of the AISI 321 steel (electron scanning microscopy) after carburizing at a depth of 2 mm.

lines in the AISI 321 steel subjected to carburizing. The possible reason for this is the redistribution of carbon atoms as a result of deformation aging due to the migration of interstitial (carbon) atoms located in solid solution to dislocations and the formation of Cottrell atmospheres. Electron microprobe analysis showed that the total carbon content on the carburized steel surface, which was measured in the grain body, increased to 1.74 wt %, in contrast to 0.66 wt % (according to XRD analysis). The maximum observed carbon content in austenitic steel of a similar chemical composition was 4.74 wt % after the low temperature gas carburizing of thin foils at 380°C [25].

Figure 5 presents the measured microhardness of the AISI 321 steel surface. The figure suggests that the microhardness of the steel after carburizing increases from 200 to 800 $HV_{0.025}$, which is comparable to that of the steel with a high content of α' martensite in the surface layer after severe surface plastic deformation [6, 13].

Since the α'-martensite content in the steel after carburizing is about 14 vol % (see Table 1), it may be argued that the high carbon concentration in the surface steel layer makes a significant contribution to the strengthening. The total depth of the hardened layer of AISI 321 austenitic steel subjected to liquid carburizing at 780°C was 2 mm. Figure 6 shows that even $Cr_{23}C_6$ chromium carbides are retained at this depth, however, the number of carbides located at grain boundaries decreases with the distance from the sample surface. For example, the low-temperature carburization of the AISI 321SS steel at 500°C results in the formation of a hardened layer of a smaller depth

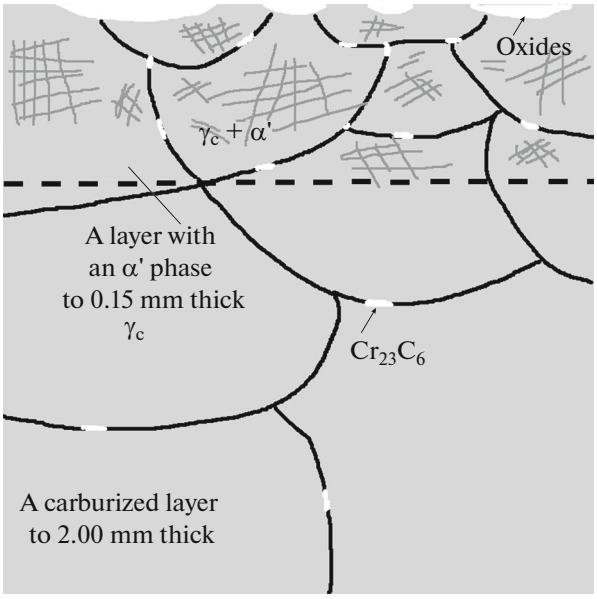

Fig. 7. Schematic structure of the AISI 321 steel surface layer after carburizing.

(0.018 mm) [26]. Figure 7 illustrates the schematic image of the surface structure of the AISI 321 steel layer after liquid carburizing at 780°C.

Optical profilometry demonstrated that the surface roughness of the quenched AISI 321 steel (polished surface) is *Ra* = 0.03 μm (Fig. 8a). Carburizing increases *Ra* parameter to 1.35 μm (Fig. 8b). This is due to the formation of deformation relief (indicated by arrow 1 in Fig. 8c) during the relaxation of thermal stresses, as well as the presence of some oxides on the surface (indicated by arrow 2 in Fig. 8c).

Thus, a decrease in the temperature of liquid carburizing to 780°C causes the formation of carbides; however, they are finely disperse and located along grain boundaries. The amount of α' martensite is also rather small and the martensite formed in the AISI 321 steel after carburizing is of deformation origin.

CONCLUSIONS

The effect of liquid carburizing at 780°C on the structure, chemical and phase composition, microhardness, and surface roughness of corrosion-resistant austenitic AISI 321 steel was investigated. The depth of the carburized layer was determined to be about 2 mm. The steel structure at a distance of 0.15 mm from the surface consisted of carbon-saturated austenite γ_c, α' martensite, and fine $Cr_{23}C_6$ chromium carbides located along austenitic grain boundaries. No carbides were observed in the grain body. There were austenite γ_c and chromium $Cr_{23}C_6$ carbides in the structure at a depth from 0.15 to 2 mm. The number and the size of carbides decrease with distance from the steel surface.

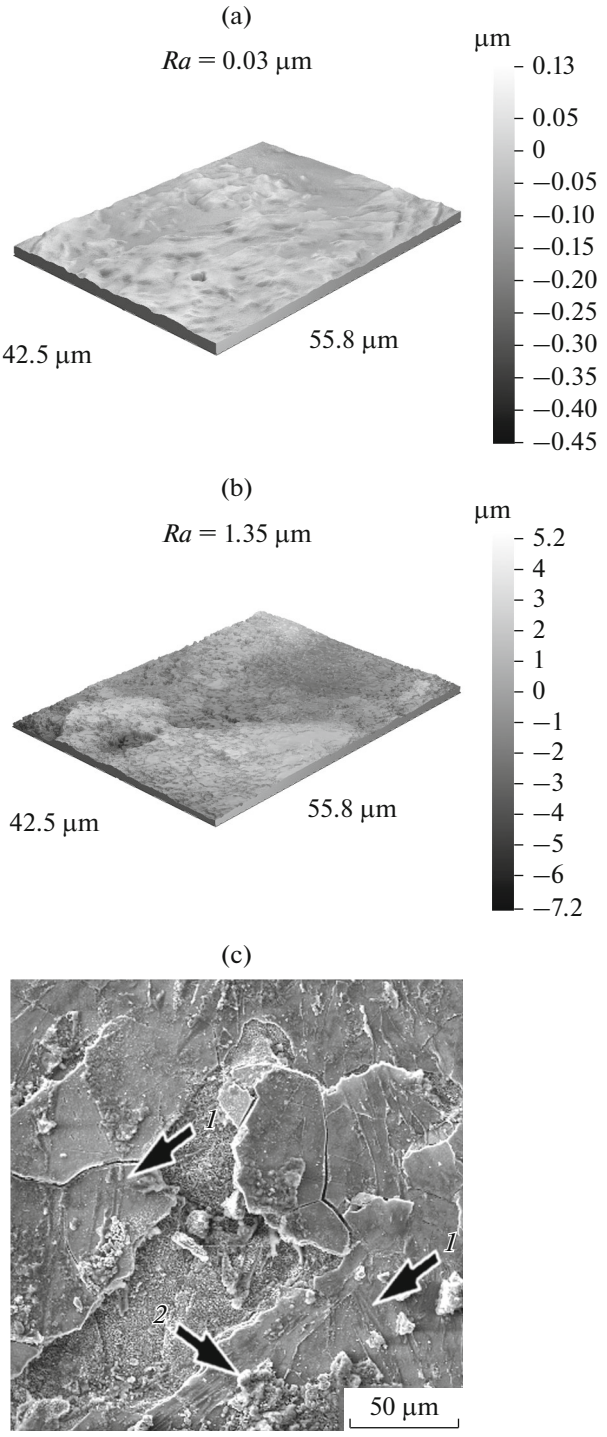

Fig. 8. AISI 321 steel surface: (a), (b) optical profilometry and (c) electron scanning microscopy; (a) in the quenched state and (b), (c) after carburizing. Arrows *1* indicate slip bands and arrow *2* indicate oxides.

Martensite formed in the AISI 321 steel after carburizing was shown to be of deformation origin. This was supported by the high dislocation density in the surface steel layer, which after carburizing increased twice as much as the dislocation density in the

quenched state. The microhardness of the AISI 321 steel surface increases by a factor of four after carburizing (from 200 to 800 $HV_{0.025}$). The high carbon concentration in the steel surface layer, which is about 1.74 wt %, makes a significant contribution to hardening. An increase in the surface roughness parameter of the carburized steel up to $Ra = 1.35$ μm is due to the formation of deformation relief and some oxides on the surface.

FUNDING

This work was performed within the state assignment of the Institute of Engineering Science, Ural Branch, Russian Academy of Sciences (theme AAAA-A18-118020790148-1) and Institute of Metal Physics, Ural Branch, Russian Academy of Sciences (theme AAAA-A18-118020190116-6) to investigate materials and select treatment conditions. It was supported in part by the Complex program of the Ural Branch, Russian Academy of Sciences (project no. 18-10-1-40) to investigate the hardness and the chemical composition of the modified surface layers.

ACKNOWLEDGMENTS

Electron scanning and optical microscopy, optical profilometry, and microhardness measurements were performed at the Center of the Collaborative Access "Plastometriya," at the Institute of Engineering Science, Ural Branch, Russian Academy of Sciences.

REFERENCES

1. M. F. McGuire, *Stainless Steels for Design Engineers* (ASM Int., 2008).
2. W. Qin, J. Kang, J. Li, W. Yue, Y. Liu, D. She, Q. Mao, and Y. Li, "Tribological behavior of the 316L stainless steel with heterogeneous lamella structure," Materials **11** (10), art. 1839 (2018).
3. R. A. Savrai, A. V. Makarov, A. L. Osintseva, and I. Yu. Malygina, "Estimating the contact endurance of the AISI 321 stainless steel under contact gigacycle fatigue tests," J. Mater. Eng. Perform. **27**, 601–611 (2018).
4. V. P. Kuznetsov, A. V. Makarov, A. L. Osintseva, A. S. Yurovskikh, R. A. Savrai, S. A. Rogovaya, and A. E. Kiryakov, "The increase of strength and surface quality of austenitic stainless steel parts by diamond burnishing on a turning/milling center," Uprochn. Tekhnol. Pokryt., No. 11, 16–26 (2011).
5. A. V. Makarov, P. A. Skorynina, A. L. Osintseva, A. S. Yurovskikh, and R. A. Savrai, "Improving the tribological properties of austenitic 12Kh18N10T steel by nanostructuring frictional treatment," Obrab. Met. (Tekhnol., Oborud., Instrum.), No. 4 (69), 80–92 (2015).
6. R. A. Savrai, A. V. Makarov, I. Yu. Malygina, S. A. Rogovaya, and A. L. Osintseva, "Improving the strength of the AISI 321 austenitic stainless steel by frictional treatment," Diagnostics, Resource and Mechanics of Materials and Structures, No. 5, 43–62 (2017). http://dream-journal.org/issues/2017-5/2017-5_149.html.
7. N. A. Narkevich, I. A. Shulepov and Yu. P. Mironov, "Structure, mechanical, and tribotechnical properties of an austenitic nitrogen steel after frictional treatment," Phys. Met. Metallogr. **118**, 399–406 (2017).
8. A. V. Makarov, P. A. Skorynina, A. S. Yurovskikh, and A. L. Osintseva, "Effect of the conditions of the nanostructuring frictional treatment process on the structural and phase states and the strengthening of metastable austenitic steel," Phys. Met. Metallogr. **118**, 1225–1235 (2017).
9. Y. Cao, F. Ernst, and G. M. Michal, "Colossal carbon supersaturation in austenitic stainless steels carburized at low temperature," Acta Mater. **51**, 4171–4181 (2003).
10. I. C. Silva, J. M. A. Rebello, A. C. Bruno, P. J. Jacques, B. Nysten, and J. Dille, "Structural and magnetic characterization of a carburized cast austenitic steel," Scr. Mater. **59**, 1010–1013 (2008).
11. F. A. P. Fernandes and L. C. C. J. Gallego, "Microstructure of nitrided and nitrocarburized layers produced on a superaustenitic stainless steel," J. Mater. Res. Technol. **2**, 158–164 (2008).
12. L. Ceschini, C. Chiavari, A. Marconi, and C. Martini, "Influence of the countermaterial on the dry sliding friction and wear behaviour of low temperature carburized AISI316L steel," Tribol. Int. **67**, 36–43 (2013).
13. A. V. Makarov, N. V. Gavrilov, G. V. Samoilova, A. S. Mamaev, A. L. Osintseva, and R. A. Savrai, "Effect of a continuous and gas-cyclic plasma nitriding on the quality of nanostructured austenitic stainless steel," Obrab. Met. (Tekhnol., Oborud., Instrum.), No. 2 (75), 55–66 (2017).
14. M. Tsujikawa, M. Egawa, T. Sone, N. Ueda, and K. Higashi, "Modification of S phase on austenitic stainless steel using fine particle shot peening steel," Surf. Coat. Technol. **228**, 318–322 (2013).
15. F. Ma, L. Pan, L. J. Zhang, Y. F. Zhu, P. Li, and M. Yang, "Structure and wear resistance of 0Cr17Ni14Mo2 austenitic stainless steel after low temperature gas carburising," Mater. Res. Innovations **18**, 1023–1027 (2014).
16. L. H. Cheng and K. S. Hwang, "Surface hardening of powder injection molded 316l stainless steels through low-temperature carburization," Metall. Mater. Trans. A **44**, 827–834 (2013).
17. P. A. Skorynina, A. V. Makarov, A. I. Men'shakov, and A. L. Osintseva, "Effect of low-temperature carburization in electron-beam plasma on the hardening and surface roughness of the metastable austenitic steel," Obrab. Met. (Tekhnol., Oborud., Instrum.) **21**, 97–109 (2019).
18. L. G. Korshunov, V. V. Sagaradze, N. L. Chernenko, and V. A. Shabashov, "Friction-induced structural transformations of the carbide phase in Hadfield steel," Phys. Met. Metallogr. **116**, 823–828 (2015).
19. R. A. Savrai, A. V. Makarov, I. Yu. Pyshmintsev, and M. A. Uimin, "Use of a magnetic method for estimating the deformation stability of retained austenite in sheet high-strength economically alloyed steels used in the automotive industry," Russ. J. Nondestr. Test. **42**, 203–207 (2006).

20. V. V. Sagaradze and A. I. Uvarov, *Strengthening and Properties of Austenitic Alloys* (RIO UrO RAN, Ekaterinburg, 2013) [in Russian].
21. G. Maistro, L. Nyborg, S. Vezzu, and Y. Cao, "Microstructural characterization and layer stability of low-temperature carburized AISI 304L and AISI 904L austenitic stainless steel," La Metallurgia Italiana, Nos. 11–12, 21–30 (2015).
22. S. R. Collins, P. C. Williams, S. V. Marx, A. Heuer, F. Ernst, and H. Kahn, "Low-temperature carburization of austenitic stainless steel" in *ASM Handbook*. Vol. 4D, *Heat Treating of Irons and Steels*, Ed. by J. Dossett and G. E. Totten, (ASM Int., 2014), pp. 451–460.
23. X. Tong, T. Zhang, and W. Ye, "Effect of carburizing atmosphere proportion on low temperature plasma carburizing of austenitic stainless steel," Adv. Mater. Mech. Ind. Eng. **598**, 90–93 (2014).
24. M. C. S. Duarte, C. Godoya, and J. C. A. B. Wilson, "Analysis of sliding wear tests of plasma processed AISI 316L steel," Surf. Coat. Technol. **260**, 316–325 (2014).
25. T. L. Christiansen, K. Ståhl, B. K. Brink, and M. A. J. Somers, "On the carbon solubility in expanded austenite and formation of Hägg carbide in AISI 316 stainless steel," Steel Res. Int. **87**, 1395–1405 (2016).
26. Y. Sun, "Kinetics of low temperature plasma carburizing of austenitic stainless steels," J. Mater. Process. Technol. **168**, 189–194 (2005).

Translated by T. Gapontseva